A novel RHH family transcription factor aCcr1 and its viral homologs dictate cell cycle progression in archaea

Yunfeng Yang[1], Junfeng Liu[1, 2 #], Xiaofei Fu[1], Fan Zhou[1], Shuo Zhang[1], Xuemei Zhang[1], Qihong Huang[1], Mart Krupovic[2], Qunxin She[1], Jinfeng Ni[1], Yulong Shen[1 #]

[1] CRISPR and Archaea Biology Research Centre, Microbial Technology Institute and State Key Laboratory of Microbial Technology, Shandong University, Qingdao, P. R. China

[2] Institut Pasteur, Université Paris Cité, CNRS UMR6047, Archaeal Virology Unit, Paris, France.

[#]Correspondence: yulgshen@sdu.edu.cn, julyjunfeng@163.com

Abstract

Cell cycle regulation is of paramount importance for all forms of life. Here we report that a transcription factor and its viral homologs control cell division in Sulfolobales. The 58-aa-long RHH (ribbon-helix-helix) family protein (designated as aCcr1) is conserved in Crenarchaeota and diverse Sulfolobales viruses. aCcr1 is essential for cell viability of *Saccharolobus islandicus* REY15A (formally *Sulfolobus islandicus* REY15A) and exhibits a cyclic transcription pattern, with the highest level being reached during active cell division (D-phase), subsequent to the expression of CdvA, an archaea-specific cell division protein. Cells over-expressing cellular aCcr1 as well as the homologs encoded by large spindle-shaped viruses *Acidianus* two-tailed virus and *Sulfolobus* monocaudavirus 3 show significant growth retardation and cell division failure, manifested as enlarged cells with multiple chromosomes. aCcr1 over-expression results in downregulation of over a dozen of genes including the *cdvA* gene. A conserved motif, aCcr1-box, located between the TATA-binding box and the translation initiation site in the promoters of 13 out of the 17 repressed genes, is critical for the aCcr1 binding. The aCcr1-box is present in the promoters of *cdvA* genes across Sulfolobales, suggesting that aCcr1-mediated *cdvA* repression is an evolutionarily conserved mechanism by which archaeal cells dictate cytokinesis progression, whereas their viruses take advantage of this mechanism to manipulate the host cell cycle.

Introduction

Cell cycle regulation is of fundamental importance for all organisms. In bacteria, cell cycle is usually divided into B (gap), C (replication), and D (growth and cell division) phases (Dewachter et al., 2018). The DNA replication, chromosome segregation, and cell division are tightly coordinated during the bacterial cell cycle, which ensures that one round of replication occurs per division event and division does not jeopardize genomic integrity. It was suggested that the coordination is achieved through either direct interaction between proteins involved in different cell cycle events or indirect coupling to cell size increase or metabolic status (Dewachter et al., 2018)(Westfall and Levin, 2017; Willis and Huang, 2017). Although cell cycle in eukaryotes is far more complex than the bacterial one, its progression is also tightly regulated, involving multiple layers of regulation. Three sets of factors were identified as the key players in the coordination of the eukaryotic cell cycle: (a) a set of cell cycle-regulated proteins including cyclin-dependent kinases (Cdk)-cyclin complexes and related kinases (Evans et al., 1983; Galderisi et al., 2003), (b) various metabolic enzymes and related metabolites, and (c) reactive-oxygen species (ROS) and cellular redox status (Diaz-Moralli et al., 2013). Cyclin-dependent kinases are the engine of sequential progression through the eukaryotic cell cycle. Cyclins bind substrates and target the Cdks to specific subcellular locations. The formation of cyclin-Cdk complex results in Cdk activation. The oscillations of the cyclins are brought about by the fluctuations in cyclin gene expression and degradation by the ubiquitin mediated proteasome

pathway (Morgan, 1995).

The mechanism underlying the cell cycle regulation in Archaea, the third domain of life, remains elusive. Two major cell division machineries are present in Archaea. Whereas euryarchaea depend on the FtsZ-based bacterial-like system, most members of the TACK superphylum, including order Sulfolobales, as well as Asgardarchaeota employ the ESCRT-III/Vps4-based cell division machinery (also called Cdv system) (Caspi and Dekker, 2018; Lindas et al., 2008; Samson et al., 2011). In halophilic euryarchaea, a ribbon-helix-helix (RHH) family transcription factor, CdrS, plays a central role in the cell division regulation (Liao et al., 2021a, 2021b). Crenarchaea, in particular, those from the Sulfolobales display eukaryotic-like cell cycle (Bernander, 2000), including a pre-replicative growth period called the G1 phase, the chromosome replication stage (S phase), a second period of cellular growth (G2 phase), and rapid genome segregation and cell division periods, known as the M and D phases, respectively (Lindas and Bernander, 2013). Cyclic gene expression patterns have been observed in the synchronized cultures of *Sulfolobus acidocaldarius* (Lundgren and Bernander, 2007). No bona fide cyclin homolog has been identified in archaea. Although some proteins possess “cyclin box” domains (e.g. transcription factor B) (Dexl et al., 2018), their functioning as genuine cyclins has not been demonstrated. Certain eukaryotic-like serine/threonine kinases, implicated in stress response in Sulfolobales species, such as *S. acidocaldarius* and *Saccharolobus islandicus* (formally *Sulfolobus islandicus*) (Hoffmann et al., 2019; Huang et al., 2020; Huang et al., 2019; Huang et al., 2017; Reimann et al., 2012), exhibit cyclic transcription patterns (Lundgren and Bernander, 2007), but their roles in cell cycle control remain to be investigated. Furthermore, Tarrason Risa et al recently reported that degradation of cell division protein ESCRT-III (CdvB) by proteasome drives cell division progression in *S. acidocaldarius* (Tarrason Risa et al., 2020). Collectively, these lines of evidence imply that Sulfolobales cells have a simplified eukaryotic-like cell cycle regulation system. Therefore, elucidation of the cell cycle regulation in Sulfolobales could provide insights into the origin and evolution of the eukaryotic cell cycle regulation.

The archaeal cell cycle is likely to be regulated, at least partly, on the transcriptional level. The archaeal transcription apparatus is a unique mixture of components from both eukaryotes and bacteria (Lemmens et al., 2019; Lewis and Stracker, 2021). Basal transcription machinery required for transcription initiation, elongation and termination is similar to that of eukaryotes and includes TATA-binding protein (TBP), transcription factor B, an RNA-Pol II-like polymerase, termination factors, and other proteins with homologs in eukaryotes (Werner and Grohmann 2011, Lemmens et al., 2019; Lewis and Stracker, 2021; Yue et al., 2020). On the other hand, the transcription regulation relies on bacterial-like transcription factors with RHH and helix-turn-helix motifs. Many archaeal transcription factors have been implicated in the regulation of metabolic processes and response to environmental stresses (Lemmens et al., 2019; Sun et al., 2018). Notably, archaea appear to encode fewer transcription factors compared to bacteria, possibly due to more complex regulation through post-translational

modifications, such as phosphorylation (Lemmens et al, 2019) and methylation (Chu et al., 2016; Vorontsov et al., 2016).

Global transcriptional analysis of *S. acidocaldarius* genome by ChIP-chip revealed cell cycle-specific transcriptional changes for 165 genes, including several transcription factors and two serine/threonine protein kinases (Lundgren and Bernander, 2007). Functional and mechanistic analysis of the corresponding proteins could help unveiling the cell cycle regulatory circuit in Sulfolobales. In this study, we identified a small RHH family transcription factor, named aCcr1 (for archaeal cell cycle regulator 1), which is essential for cell viability and involved in the control of cell division in *S. islandicus* REY15A. Over-expression of the cellular and viral aCcr1 homologs leads to cell enlargement and growth retardation. Transcriptomic analysis revealed that a number of genes, including *cdvA* and *ePK1*, are strongly downregulated in cells overexpressing aCcr1. Consistently, the purified cellular and viral aCcr1 proteins bind to the promoters of *cdvA* and *ePK1*, specifically at a conserved 9-nt motif (aCcr1-box). Our results demonstrate that aCcr1 plays a key role in cell division regulation and imply that it is also involved in the cell cycle manipulation by viruses.

MATERIALS AND METHODS

Strains and growth conditions. *Saccharolobus islandicus* REY15A was grown aerobically at 75°C in STV medium containing mineral salt, 0.2% (w/v) sucrose (S), 0.2% (w/v) tryptone (T), and a mixed vitamin solution (V). *S. islandicus* REY15A(E233S)(Δ*pyrEF*Δ*lacS*), hereafter E233S, was grown in STVU (STV supplemented with 0.01% (w/v) uracil) medium. The medium was adjusted to pH 3.5 with sulfuric acid, as described previously (Deng et al., 2009). SCV medium containing 0.2% (w/v) casamino acid (C) was used for screening and cultivating uracil prototrophic transformants. ATV medium containing 0.2% (w/v) D-arabinose (A) was used for protein expression. Culture plates were prepared using gelrite (0.8% [w/v]) by mixing 2×STV and an equal volume of 1.6% gelrite. The strains constructed and used in this study are listed in the Supplementary information (Table S1).

Phase contrast and immunofluorescence microscopy. For microscopy analysis, 5 μl of cell suspension at the indicated time points were examined under a NIKON TI-E inverted fluorescence microscope (Nikon Japan). Immunofluorescence microscopy analysis was carried out as previously described (Liu et al., 2021b). Briefly, *S. islandicus* REY15A cells were collected and pelleted down at 6,000 rpm for 5 min, re-suspended in 300 μl PBS buffer (137 mM NaCl, 2.7 mM KCl, 10 mM Na_2HPO_4 $12H_2O$, 2 mM KH_2PO_4, pH7.4), and fixed by addition of 700 μl cold absolute ethanol and kept at 4°C for at least 2 h. The fixed cells were washed for 3 times with PBST (PBS plus 0.05% Tween-20) to remove ethanol. Primary antibodies against ESCRT-III (HuaAn Biotechnology Co., Hangzhou, Zhejiang, China) were added with a dilution of 1:1,000 in PBST and incubated at 4 °C overnight. The cells were washed 3 times and then incubated with the goat anti-rabbit secondary antibodies Alexa Fluor® 488 (1:1,000,

148 Thermo Fisher Scientific, USA) for ESCRT-III, and Concanavalin A Alexa Fluor 647
149 Conjugate (50 μg/ml, Invitrogen™, Thermo Fisher Scientific, USA) for S-layer, and
150 kept at 4 °C for 2-4 h. The localization of ESCRT-III was observed under a SP8
151 confocal microscope, and the data were analysed using Leica Application Suite X (LAS
152 X) software (Leica).

153 **Flow cytometry analysis.** The procedure for the flow cytometry analysis followed the
154 reported method (Liu et al., 2021a, 2021b). Briefly, approximately 3×10^7 cells were
155 collected for flow cytometry analysis. Cells were harvested at the indicated time points
156 and fixed with 70% cool ethanol overnight (>12 h). The fixed cells were then pelleted
157 at 2,800 rpm for 20 min. The cells were re-suspended and washed with 1 ml of PBS
158 buffer. Finally, the cells were pelleted again and resuspended in 100 μl of staining
159 buffer containing 50 μg/ml propidium iodide (PI) or SuperGreen. After staining for 30
160 min, the DNA content was analysed using the ImageStreamX MarkII Quantitative
161 imaging analysis for flow cytometry system (Merck Millipore, Germany), which was
162 calibrated with non-labelled beads with a diameter of 2 μm. The data from at least
163 20,000 cells were collected for each sample and the data of the single cells were
164 analysed with the IDEAS software.

165 **Transcriptome analysis.** Strains of Sis/pSeSD and Sis/pSeSD-aCcr1 were cultured
166 in ATV medium under the conditions as described above. For transcriptomic analysis,
167 culture was inoculated with an initial OD_{600} of 0.05. The cells were pelleted at 7,000
168 rpm for 10 min after 12 h of cultivation when the OD_{600} reached approximately 0.2. The
169 pellet was resuspended in 1 ml PBS buffer. The cells were pelleted again and stored
170 at -80°C. Total RNA was extracted using the Trizol reagent (Ambion, Austin, TX, USA).
171 Total amounts and the integrity of RNA were assessed using the RNA Nano 6000
172 Assay Kit of the Bioanalyzer 2100 system (Agilent Technologies, CA, USA).
173 Transcriptomic analysis was performed by Novogene (Beijing, China). About 3 μg of
174 high-quality RNA per sample was used for the construction of RNA-Seq libraries. The
175 libraries are sequenced by the Illumina NovaSeq 6000. Clean reads were aligned to
176 the reference genome sequence of *S. islandicus* REY15A (Guo et al., 2011). The
177 resulting data were then analysed by Fragments Per Kilobase of transcript sequence
178 per Million base pairs sequenced (FPKM) analysis to reveal expression levels of all
179 genes in the *S. islandicus* genome. Differential genome expression analysis (over-
180 expression of aCcr1 versus empty vector) was performed using the DEGSeq R
181 package. The resulting P-values were adjusted using the Benjamini and Hochberg's
182 approach for controlling the false discovery rate padj<0.05 and |log2(foldchange)| > 0
183 were set as the threshold for significantly differential expression.

184 **Cell cycle synchronization.** *S. islandicus* REY15A cells were synchronized as
185 previously described (Liu et al., 2021a; Liu et al., 2021b) with slight modifications.
186 Briefly, cells were first grown aerobically at 75°C with shaking (145 rpm) in 30 ml of
187 STV medium. When the OD_{600} reached 0.6-0.8, the cells were transferred into 300 ml
188 STV medium with an initial estimated OD_{600} of 0.05. When the OD_{600} reached 0.15-0.2,

acetic acid was added at a final concentration of 6 mM and the cells were blocked at G2 phase of the cell cycle after 6h treatment. Then, the cells were collected by centrifugation at 3,000 *g* for 10 min at room temperature to remove the acetic acid and washed twice with 0.7% (w/v) sucrose. Finally, the cells were resuspended in 300 ml of pre-warmed STV medium and cultivated as above for subsequent analysis.

Quantitative reverse transcription PCR (RT-qPCR). Samples from the control and the aCcr1-over-expression strains were collected at indicated time points (same as for the transcriptome analysis). Total RNA was extracted using SparkZol (SparkJade Co., Shandong, China). First-strand cDNAs were synthesized from the total RNA according to the protocol of the First Strand cDNA Synthesis Kit (Accurate Biotechnology Co., Hunan, China) for RT-qPCR. The resulting cDNA preparations were used to evaluate the mRNA levels of the target genes by qPCR using the SYBR Green Premix Pro Taq HS qPCR Kit (Accurate Biotechnology Co., Hunan, China) and the gene specific primers (Table S2). PCR was performed in an CFX96^{TM} (Bio-Rad) with the following steps: denaturing at 95℃ for 30s, 40 cycles of 95℃ 5s, 60℃ 30s. Relative amounts of mRNAs were evaluated using the comparative Ct method with 16S rRNA as the reference.

Protein purification and chemical cross-linking. To purify the wild-type aCcr1 (SiRe_0197) and its mutant proteins from *E. coli,* cells harbouring plasmids pET22b-aCcr1-C-His, pET22b-aCcr1-R2A-C-His, pET22b-aCcr1-K7A-C-His, pET22b-aCcr1-R27A-C-His, pET22b-ATV_gp29-C-His, pET22b- SIRV2_gp21-C-His, pET22b-SMV3_gp63-C-His, and pET22b-STIV2_B60-C-His were grown in 2 litres of LB medium at 37°C with shaking until the optical density OD_{600} reached 0.4~0.6, when 1.0 mM IPTG was added into the cultures and the cells were then grown at 37°C for 4 h with shaking. The cells were harvested by centrifugation at 7,000 *g* for 10 min and then resuspended in the lysis buffer A (50 mM Tris-HCl [pH 7.4], 200 mM NaCl, and 5% glycerol). Then, the cells were crushed with an ultrasonic crusher and cell debris was removed by centrifugation at 12,000 *g* for 15 min. The supernatant was incubated at 70°C for 20 min, centrifuged, and then filtered through a membrane filter (0.45 μm). The samples were loaded onto a Ni-NTA agarose column (Invitrogen) pre-equilibrated with buffer A. Finally, the target protein was eluted with buffer A containing 300 mM imidazole. The eluted sample was analysed using a 18% SDS-PAGE gel. The protein samples were concentrated by ultrafiltration using an Amicon Ultra-3KDa concentrator (Millipore). For further purification, size exclusion chromatography was performed using a Superdex 200 increase 10/300 column (GE Healthcare). The protein concentration was determined by the Bradford method using bovine serum albumin as the standard. To assay the oligomeric status, the wild type aCcr1 protein was incubated with increasing concentrations of glutaraldehyde (0.01 to 0.16%) on ice at 4°C for 15 min. The reaction was then stopped by the addition of SDS-PAGE loading buffer, after which the samples were electrophoresed by 20% SDS–PAGE, and the gel was stained with Coomassie blue R-250.

Western blotting. Antibodies against TBP, CdvA and ESCRT-III were produced using synthetic specific peptides (amino acids 18-31, SIPNIEYDPDQFPG for TBP (SiRe_1138); 13-25, GQKVKDIYGREFG for CdvA (SiRe_1173); 194-208 IEQSSRVSQSRPAVR for ESCRT-III (SiRe_1174)). Antibody against SisCcr1 (Ccr1 from *Sulfolobus islandicus* REY15A) was produced using purified recombinant proteins purified from *E. coli*. Antibodies against TBP, CdvA and aCcr1 were produced in rabbit, and CdvA in rat. All the antibodies were produced by HuaAn Biotechnology Co. (Hangzhou, Zhejiang, China). For standard Western blotting analysis, 2×10^8 cells (with or without induction) at the indicated times were collected by centrifugation at 5,000 *g* for 10 minutes and resuspended in 20 μl PBS buffer. After the addition of 5 μl 5× loading buffer, the samples were treated at 100 ℃ for 10 minutes and analysed by SDS-PAGE. The proteins in the PAGE gel were transferred onto a PVDF membrane at 30 mA for 16 h at 4℃. Membranes were blocked with 5 % (w/v) skimmed milk for 2 h at room temperature. The membrane was washed and incubated with a primary antibody and then the secondary anti-rabbit HRP conjugate antibody (TransGen Biotech company, Beijing, China) following the standard protocol. Finally, the membranes were imaged using an Amersham ImageQuant 800 biomolecular imager (Cytiva).

Electrophoretic mobility shift assay (EMSA). Substrates used in EMSA experiments were generated by annealing the complementary oligonucleotides with 5'FAM-labelled oligonucleotides (Table S2). The reaction mixture (20 μl) containing 2 nM of the FAM-labelled substrates and different concentrations of aCcr1 or the mutant proteins was incubated at 37℃ for 30 min in binding buffer (25 mM Tris–HCl, pH8.0, 25 mM NaCl, 5 mM $MgCl_2$, 10% glycerol, 1 mM dithiothreitol). After the reaction, samples were loaded onto a 10% native PAGE gel buffered with 0.5× Tris–borate–EDTA (TBE) solution. DNA–protein complexes were separated at 200 V for 60 min. The resulting fluorescence was visualized by an Amersham ImageQuant 800 biomolecular imager (Cytiva).

Phylogenetic analysis. aCcr1 homologs were collected by PSI-BLAST (2 iterations against the RefSeq database at NCBI; E=1e-05) (Altschul et al., 1997). The collected sequences were then clustered using MMseq2 (Gabler et al., 2020) to 90% identity over 80% of the protein length. Sequences were aligned using MAFFT v7 (Katoh et al., 2019) and the resultant alignment trimmed using trimal (Capella-Gutierrez et al., 2009), with the gap threshold of 0.2. Maximum likelihood phylogenetic analysis was performed using IQ-Tree (Minh et al., 2020), with the best selected amino acid substitution model being LG+I+G4. The branch support was assessed using SH-aLRT (Guindon et al., 2010).

Chromatin immunoprecipitation (ChIP-seq). Chromatin immunoprecipitation (ChIP-seq) was performed according to Naomichi et al. (2019) with slight modifications. Briefly, the cells were collected 3 hours after synchronization, cross-linked by adding 1% formaldehyde for 15 minutes, and quenched with a final concentration of 125 mM

glycine. The cells were pelleted by centrifugation at 5,000 *g* for 10 minutes and washed with PBS. The cells were then resuspended in TBS-TT buffer (20 mM Tris, 150 mM NaCl, 0.1% Tween-20, 0.1% Triton X-100, pH 7.5) and fragmented by sonication until the DNA fragments were of 200-500 bp. After centrifugation (10,000 *g* for 15 minutes), a 100 μl aliquot of the DNA-containing supernatant was kept apart to use as an input control and the remaining sample was divided into two aliquots. One aliquot was incubated with anti-aCcr1 antibody-coated protein A beads (Cytiva) and the other was incubated with pre-immune serum-coated protein A beads, which served as a nonspecific binding control (Mock control). After incubation at 60 °C for 10 hrs, the samples were collected and the captured DNA was purified by using the DNA Cycle-Pure Kit (Omega) according to the manufacturer's instruction. The input samples were treated as above without the addition of antiserum and beads. The purified DNA was used for ChIP-seq library preparation. The library was constructed by Novogene Corporation (Beijing, China). Subsequently, pair-end sequencing of sample was performed on Illumina platform (Illumina, CA, USA). Library quality was assessed on the Agilent Bioanalyzer 2100 system.

Results

The cyclically transcribed gene *aCcr1* is essential for cell viability

A previous genome-wide transcriptomic analysis by microarray revealed seven transcription factors which displayed cyclic expression patterns in *S. acidocaldarius* (Lundgren and Bernander, 2007). These include one of the three eukaryotic transcription initiation factor IIB homologs, Tfb2 (Saci_1341), an RHH domain protein (CopG family, Saci_0942), a DtxR family protein (Saci_1012), a Tet family protein (Saci_1107), an Lrp/AsnC family protein (Saci_2136), and two HTH domain-containing proteins (Saci_0102 and Saci_0800). Except for the Tet and Lrp/AsnC family proteins, these transcription factors are conserved in *S. islandicus* REY15A, suggesting that they play important roles in cell cycle regulation. To test this hypothesis, we focused on SiRe_0197, an RHH domain protein of *S. islandicus* REY15A. We name it aCcr1 (for archaeal Cell cycle regulator 1) based on the results described below.

aCcr1 is a 58-amino acid protein (Fig. S1A) with an isoelectric point of 9.45 and a predicted molecular mass of 6.9 kDa. Similar to other RHH proteins, aCcr1 is predicted to function as a dimer (Schreiter and Drennan, 2007) and interact with the major groove of the dsDNA via a two-stranded β-sheet containing positively charged amino acid residues (Fig. S1B). Indeed, we confirmed that the purified aCcr1 protein existed as a dimer in solution using size exclusion chromatography and glutaraldehyde cross-linking (Fig. S2A and S2B).

Transcriptomic analysis of cell cycle-synchronized *S. islandicus* REY15A cells (Liu et al., 2021b) revealed that the transcription levels of *aCcr1* and cell division genes *cdvA*, *escrt-III*, and *vps4* exhibit cyclic patterns (Fig. 1). Interestingly, the transcriptional level

310 of *cdvA* peaked at about 60 minutes following the removal of acetic acid, which was
311 used to synchronize the cells in G2 phase, while the levels of *aCcr1*, *escrt-III* and *vps4*
312 reached their maxima at approximately 120 minutes after the release of the cell cycle
313 arrest. This result is consistent with that based on microarray analysis in *S.*
314 *acidocaldarius* (Lundgren and Bernander, 2007) and indicates that aCcr1 (SiRe_0197)
315 is likely a cell division specific transcription factor in *S. islandicus* REY15A.

316 To verify the importance of aCcr1 for the cell, we attempted to knock out *aCcr1* using
317 an endogenous CRISPR-based genome editing system in *S. islandicus* REY15A (Fig.
318 S3, Li et al., 2016). However, all attempts failed to yield any viable knockout clones,
319 implying that *aCcr1* is an essential gene. This result suggests that the putative
320 regulatory role of aCcr1 is indispensable for cell survival.

321 **The DNA binding activity of aCcr1 is critical for its cell division regulation**

322 To probe the *in vivo* function of aCcr1, we attempted to obtain strains with aCcr1 being
323 down- or up-regulated. Unfortunately, there was no suitable protospacer in *aCcr1* of *S.*
324 *islandicus* REY15A, precluding CRISPR-based knockdown strategy (Li et al., 2016;
325 Peng et al., 2017). However, to facilitate the functional analysis of aCcr1, a series of
326 aCcr1 over-expression strains, including those over-expressing the wild type aCcr1 as
327 well as putative DNA-binding deficient mutants aCcr1(R2A), aCcr1(K7A), and
328 aCcr1(R27A) (Fig. S1B), were obtained (Table S1).

329 Compared to the control, cells over-expressing aCcr1 showed an obvious growth
330 retardation (Fig. 2A) and exhibited greatly enlarged cell sizes (Fig. 2B and 2C) and
331 increased amounts of DNA (Fig. 2D). The average diameter of the cells reached a
332 maximum of 4.58 μm at 24 h after induction (Fig. 2C). These phenotypes are indicative
333 of cell division defects in cells over-expressing aCcr1. To verify that the observed cell
334 division defect is dependent on the DNA binding activity of aCcr1, we compared the
335 growth and cell sizes of the strains over-expressing the wild type aCcr1 and DNA-
336 binding deficient mutants R2A, K7A, and R27A. As shown in Fig. S4A-4C, all the cells
337 over-expressing the mutant proteins displayed normal growth and cell morphology.
338 The expression of the wild type and mutant aCcr1 proteins was confirmed by Western
339 blotting analysis (Fig. S4D). These results indicated that the positively charged
340 residues play a critical role in the regulation of target gene expression and suggests
341 that the DNA binding activity is essential for cell division regulation.

342 **The cell division gene *cdvA* is strongly downregulated in cells over-expressing**
343 **aCcr1**

344 To identify which genes are transcriptionally regulated by aCcr1 and to gain insight
345 into how aCcr1 over-expression influences cell division, we conducted comparative
346 transcriptomic analysis of the aCcr1 over-expressing strain and the control carrying
347 an empty vector pSeSD. Samples were taken at 12 h after arabinose induction and

348 subjected to transcriptomic analysis. In total, 76 and 124 genes were up- and
349 downregulated by more than two folds, respectively (Table S3-S4, Fig. 3). Taking 4-
350 fold change as a threshold, 4 and 17 genes were up- and down-regulated,
351 respectively (Fig. 3, Table 1). Intriguingly, *cdvA* (*sire_1173*), the archaea-specific cell
352 division gene (Lindas et al., 2008; Liu et al., 2017; Samson et al., 2008), was among
353 the most highly down-regulated genes (Fig. 3, Table 1). During cell division, CdvA
354 binds to the chromosome and membrane, forming the ring-like structure, then
355 recruits ESCRT-III to the mid-cell for cell division (Moriscot et al., 2011; Samson et
356 al., 2011). Over-expression of aCcr1 leads to increase in cell diameter and DNA
357 content, indicative of failure in cell division. A very similar phenotype was obtained
358 when *cdvA* transcription was downregulated using the CRISPR knockdown
359 technology (Liu et al., 2021b). In addition, the gene coding for ePK1 (SiRe_2056), a
360 eukaryotic-like serine/threonine protein kinase, was also among the significantly
361 down-regulated genes (Fig. 3, Table 1).

362 **Ccr1 binds to the promoters of *cdvA* and other highly down-regulated genes at**
363 **a conserved motif, aCcr1-box**

364 To test whether aCcr1 binds to the promoter of *cdvA*, we performed the electrophoresis
365 mobility shift assay (EMSA) using P_{cdvA} as a substrate. Purified aCcr1 protein (0, 0.1,
366 0.2, 0.4, and 0.8 μM) was incubated with fluorescein (FAM)-labelled DNA substrates
367 (Fig. 4A). When an oligonucleotide with the sequence corresponding to the distal
368 region (-100 to -51) of the P_{cdvA} promoter was used as a substrate, no retardation in
369 electrophoretic mobility was observed (Fig. 4A and 4C). In contrast, when the substrate
370 contained the P_{cdvA} sequence proximal to the first *cdvA* codon (-50 to -1),
371 electrophoretic mobility was retarded in a protein concentration dependent manner
372 (Fig. 4A and 4C). Therefore, the aCcr1 binding site was localized to the -50 to -1 region,
373 covering the BRE (TFB recognition element), TATA-box, and the TSS (transcription
374 start site) regions. To further characterize the DNA binding activity of aCcr1, we
375 expressed and purified the site-directed mutants of aCcr1, aCcr1(R2A), aCcr1(K7A),
376 and aCcr1(R27A), from *E. coli* (Table S1, Fig. S1B and S5A). All the mutants lost the
377 ability to bind to the *cdvA* promoter (Fig. S5B). Thus, we confirmed that R2, K7, and
378 R27 are critical for promoter binding. In addition, we found that aCcr1 was also able to
379 bind to P_{sire_2056}, a promoter regulating the expression of ePK1-encoding gene
380 *sire_2056* (Fig. S5D).

381 To understand the substrate binding specificity of aCcr1, we analysed the promoter
382 sequences of all 17 genes repressed in the aCcr1 over-expression strain (Tables 1-2,
383 Fig. 5). Notably, *sire_0018* and *sire_0019* are within the same operon, and so are
384 *sire_0623* and *sire_0624*, whereas a bidirectional promoter sequence is apparently
385 shared by *sire_2056* and *sire_2057* (Fig. 5). All 15 promoter sequences of aCcr1-
386 repressed *S. islandicus* REY15A genes were retrieved and subjected to de novo motif
387 discovery by MEME server. We found that 10 promoters (of 12 genes) contain one or

388 two copies of a 9 bp motif A(T/G)G(A)TA(G)A(T/G)TACN, which we name as aCcr1-
389 box (Fig. 4B and Fig. 5, Table 2).

390 We confirmed the importance of the motif for aCcr1 binding to the promoters of c*dvA*
391 by EMSA. As shown in Fig. 4C and 4D, deletion of either one aCcr1-box reduced the
392 binding affinity, while deletion or replacement of both motifs greatly impaired the
393 binding of aCcr1. Interestingly, aCcr1-boxes are present in the promoters of *cdvA*
394 homologs from other Sulfolobales species, e.g., *S. acidocaldarius* DSM639
395 (*saci_1374*), *Acidianus hospitalis* W1 (*ahos_1333*), *Metallosphaera cuprina* Ar-4
396 (*mcup_0558*), *Sulfuracidifex tepidarius* (*ic006_1093*), and *Stygiolobus azoricus*
397 (*d1868_04805*) (Table 2), suggesting that aCcr1 binding to *cdvA* promoter is
398 conserved in Sulfolobales. To test if the aCcr1 homologs from other crenarchaeal
399 species are functional *in vivo*, we over-expressed in *S. islandicus* REY15A SacCcr1
400 (Ccr1 from *S. acidocaldarius*), which differs from SisCcr1 by four residues (Y23T, M38L,
401 L43T, and R47T) (Fig. S1A). As expected, the SacCcr1 over-expression strain showed
402 similar phenotype to cells over-expressing SisCcr1 (Fig. S7). Given that aCcr1-box
403 motifs are present in the promoters of *cdvA* genes across Sulfolobales (Table 2), the
404 mechanism of aCcr1-mediated control of cell division through repression of CdvA is
405 likely to be conserved as well, at least, in members of the Sulfolobales. We also found
406 that the motif in the promoter of *ePK1* (*sire_2056*) is critical for aCcr1 binding (Fig.
407 S5D). Consistent with the above results, chromatin immunoprecipitation sequencing
408 (ChIP-seq) analysis has shown that the promoter regions of *cdvA* and *ePK1* are also
409 highly enriched in aCcr1 in *vivo* (Fig. S8). Thus, 13 out of 17 genes with more than 4-
410 fold downregulation could be repressed by aCcr1 binding to the aCcr1-box motif within
411 their promoters. Because most of the sites are located between the TATA-box and the
412 translation start site, binding to the promotor by aCcr1 would prevent the formation of
413 translational pre-initiation complex, leading to transcription repression. While the
414 repression of *cdvA* by aCcr1 is probably the main mechanism for cell division failure in
415 the aCcr1 over-expression strain, the physiological functions of repression of other
416 genes such as *ePK1* by aCcr1 need further investigation.

417 **Over-expression of aCcr1 affects cell cycle progression due to specific**
418 **downregulation of *cdvA* and other cell division genes**

419 The growth retardation and cell enlargement phenotypes of the aCcr1 over-expression
420 strain suggested that the cell division genes could be downregulated. Cell division in
421 Sulfolobales is dependent on the eukaryotic-like ESCRT machinery, which comprises
422 the archaea-specific protein CdvA, four ESCRT-III homologs (ESCRT-III [CdvB],
423 ESCRT-III-1 [CdvB1], ESCRT-III-2 [CdvB2], ESCRT-III-3 [CdvB3]), and an AAA+
424 ATPase Vps4 (also known as CdvC) (Lindas et al., 2008; Liu et al., 2017; Samson et
425 al., 2008). CdvA binds to DNA and membrane (Moriscot et al., 2011; Samson et al.,
426 2011) and then recruits ESCRT-III to the mid-cell, where it forms a ring-like structure
427 and drives cell division (Samson et al., 2011). Vps4 binds to ESCRT-III and other
428 ESCRT-III homologs (Liu et al., 2017) and, upon ATP hydrolysis, drives the

429 disassembly of the contractile ESCRT-III ring, thereby promoting the cell division
430 process (Samson et al., 2008; Tarrason Risa et al., 2020). In a previous study, we
431 reported that infection of *S. islandicus* REY15A with virus STSV2 led to transcriptional
432 downregulation of cell division genes, including *cdvA*, *escrt-III, escrt-III-1, escrt-III-2,*
433 *escrt-III-3* and vps4, which resulted in dramatic increase in the size and DNA content
434 of infected cells (Liu et al., 2021a). To confirm the role of aCcr1 in cell division
435 regulation and to investigate the effect of aCcr1 over-expression on cell division
436 proteins, we examined the relative transcriptional levels of the corresponding genes
437 by RT-qPCR. As shown in Fig. 6A, all of the above mentioned cell division genes were
438 significantly repressed. Among them, *cdvA* was affected most strongly. To detect if
439 aCcr1 over-expression also affects the expression of genes in the upstream cell cycle
440 process, we examined the expression levels of chromosome segregation genes *segA*
441 and *segB* (Yen et al., 2021), but no significant changes were found (Fig. 6B),
442 suggesting that over-expression of aCcr1 does not affect the process of chromosome
443 segregation.

444 To further confirm the regulatory role of aCcr1 in cell cycle progression, we analysed
445 the aCcr1 over-expression strain by flow cytometry using synchronized cells. We
446 added D-arabinose 3 h after the addition of acetic acid (Fig. 7A). The expression of
447 aCcr1 was induced 1.0 h before the acetic acid was removed, as confirmed by Western
448 blotting. *S. islandicus* REY15A (E233S) containing the empty plasmid was used as a
449 control. As shown in Fig. 7B, subpopulation of cells containing a single chromosome
450 copy (1C) could be observed at 0-4 h and up to the end of the normal cell cycle in the
451 control, but not in the aCcr1 over-expression strain. Thus, over-expression of aCcr1
452 inhibited cell division. Western blotting results showed that in the control cells, CdvA
453 exhibited a cyclic pattern with higher expression at 0-1 h (Fig. 7C). In contrast, the
454 CdvA levels remained low in the aCcr1 over-expression cells, consistent with the RT-
455 qPCR results. Thus, we established that binding of aCcr1 to the promoter of *cdvA*
456 represses the gene expression and reduces CdvA level in the cell, leading to cell
457 division failure.

458 **Ccr1 over-expression jeopardizes contractile ring formation**

459 To further characterize how the cell division is affected by the over-expression of aCcr1,
460 we performed fluorescence microscopy analysis on the synchronized cells over-
461 expressing aCcr1 using anti-ESCRT-III antibodies. Cells cultured at 3-4 h after removal
462 of acetic acid were sampled and analysed. In the control cells carrying the empty vector,
463 ESCRT-III displayed mid-cell localization and formed ring-like structures in 7.2% of the
464 cells (Fig. 7D). In the aCcr1 over-expressing strain, ESCRT-III ring was barely visible
465 (0.8%), probably because in the absence of CdvA, ESCRT-III cannot be recruited to
466 the membrane (Fig. 7D). This result further reinforces the hypothesis that aCcr1
467 regulates cell division via *cdvA* repression.

468 **Ccr1 homologs are widespread in Sulfolobales and their viruses**

469 To explore the diversity and distribution of aCcr1 in the domain Archaea, we performed
470 PSI-BLAST search using aCcr1 from *S. islandicus* REY15A as a query. Given that
471 RHH domain proteins are widespread in archaea and orthology of short divergent
472 proteins is not straightforward to assess, we restricted our focus to proteins displaying
473 relatively high sequence similarity to aCcr1 and retrievable after two iterations of PSI-
474 BLAST. The search yielded multiple hits in hyperthermophilic crenarchaea of the
475 orders Sulfolobales and Desulfurococcales (Fig. 8). We note, however, that further
476 search iterations revealed additional homologs in a broader diversity of archaea,
477 including those from other phyla. In Sulfolobales genomes, aCcr1 genes are encoded
478 within orthologous loci and have conserved gene synteny (Fig. S6). Interestingly, all
479 *cdvA* promoter sequences of the Sulfolobales species contain at least one aCcr1-box
480 motif at a conserved position (Table 2).

481 Intriguingly, aCcr1 homologs are also conserved in several conjugative plasmids and
482 genomes of Sulfolobales viruses from five different families, including *Rudiviridae*,
483 *Bicaudaviridae*, *Fuselloviridae*, *Ungulaviridae* and *Turriviridae* (Prangishvili et al., 2017)
484 as well as in unclassified Sulfolobales viruses YNP1 and YNP2 (Fig. 8). The viral,
485 plasmid and cellular aCcr1 homologs display a complex evolutionary history with
486 multiple horizontal gene transfers, even within the same family of viruses. The
487 phylogeny splits into three major clades (I-III), with members of the Sulfolobales being
488 distributed between clades I and III, and Desulfurococcales forming the clade II (Fig.
489 8). Viruses are intermixed with the Sulfolobales within clades I and III, whereas
490 plasmids are restricted to clade III. The horizontal gene transfer of aCcr1 homologs
491 between viruses and cells suggests that viruses might have hijacked aCcr1 genes for
492 manipulation of the cell cycle of their hosts on multiple occasions.

493 **Over-expression of viral aCcr1 homologs impairs cell cycle progression in *S.***
494 ***islandicus* REY15A**

495 To investigate the functions of viral aCcr1 homologs, we have chosen four viruses
496 belonging to clade I, which also includes aCcr1 of *S. islandicus* REY15A and *S.*
497 *acidocaldarius* (Fig. 8). In particular, we constructed strains over-expressing aCcr1
498 homologs from *Acidianus* two-tailed virus (ATV_gp29), *Sulfolobus* monocaudavirus 3
499 (SMV3_gp63), *Sulfolobus islandicus* rod-shaped virus 2 (SIRV2_gp21), and
500 *Sulfolobus* turreted icosahedral virus 2 (STIV2_B60). The former two viruses belong
501 to the same family as STSV2, which has been recently demonstrated to induce cell
502 enlargement upon infection (Liu et al., 2021a), while the latter two are lytic viruses that
503 do not induce obvious cell size alterations (Happonen et al., 2010; Kessler et al., 2004)
504 Over-expression of the ATV_gp29 and SMV3_gp63 resulted in growth retardation and
505 yielded enlarged cells with multiple chromosomes (Fig. 9, S9C), reminiscent of the cell
506 phenotype induced by STSV2 and SMV1 infections (Liu et al., 2021a). By contrast, the
507 growth of transformants carrying plasmids pSeSD-SIRV2_gp21 and pSeSD-
508 STIV2_B60 homologs, respectively, did not have apparent effect on the cell growth
509 and morphology (Fig. S9A and S9B). We thus checked the protein expression in the

510 strains carrying each of the four plasmids by Western blotting and found that the
511 proteins were indeed expressed, except for SIRV2_gp21 (Fig. S9C). We then checked
512 the binding activity of the four proteins to a DNA fragment containing P_{cdvA}. Purified
513 ATV_gp29, SMV3_gp63, and SIRV2_gp21 proteins (expressed in *E. coli)* could bind
514 to the P_{cdvA} promoter, whereas STIV2_B60 could not (Fig. S5C). Careful examination
515 of the amino acid sequence of STIV2 showed that one of the putative DNA binding site
516 arginines (R2) is replaced with glutamine (Fig. S1A), which may explain why
517 STIV2_B60 did not bind to P_{cdvA}. Thus, these results suggest a mechanism by which
518 viruses, particularly, bicaudaviruses, can control the division of their host cells. By
519 using a small RHH family cell division regulator, probably obtained by horizontal gene
520 transfer from their hosts, the viruses can manipulate the cell cycle, transforming the
521 cell into a giant virion producing factory for viral production.

522 **Discussion**

523 Studies on the cell cycle progression and regulation in archaea could provide a key to
524 understanding the eukaryogenesis, one of the most intriguing mysteries in biology.
525 Recent research has shown that archaea of the Asgard superphylum, in particular,
526 Heimdallarchaeota, are evolutionarily most closely related to eukaryotes (Imachi et al.,
527 2020; Liu et al., 2021c; Zaremba-Niedzwiedzka et al., 2017). However,
528 microorganisms from the Asgard superphylum are difficult to cultivate and no
529 genetically tractable system has been established, which hinders the characterization
530 of the putative archaeal ancestor of eukaryotes. Archaea of the TACK superphylum
531 share many features with the Asgard superphylum and could serve as valuable models
532 for understanding the evolution of eukaryotic-like features in archaea. In particular,
533 genetically tractable members of the genera *Sulfolobus* and *Saccharolobus* represent
534 one of such archaeal model systems with many eukaryotic signature proteins and a
535 eukaryotic-like cell cycle (Bernander and Poplawski, 1997; Spang et al., 2017).
536 Mapping of cell cycle regulatory mechanisms and identification of proteins involved in
537 cell-cycle processes in these model archaea is crucial for understanding the basic
538 biology of archaea (Lundgren and Bernander, 2007) and the origin of Eukaryota. In
539 this study, we identified a small RHH family transcription factor, named aCcr1, from
540 Sulfolobales and their viruses that can control the cell division of *S. islandicus*. It binds
541 to a conserved 9-bp palindromic motif, aCcr1-box, within the promoter of *cdvA*, an
542 archaea-specific component of the cell division machinery, thereby repressing the
543 *cdvA* expression. Notably, sequence analysis showed that the aCcr1-box is present in
544 all Sulfolobales *cdvA* promoters at equivalent positions. Thus, we hypothesize that
545 aCcr1-mediated cell cycle control through repression of CdvA is conserved in this
546 archaeal order.

547 In euryarchaea, the FtsZ-based bacterial-like system is utilized for the cell division
548 (Caspi and Dekker, 2018; Lindas et al., 2008; Samson et al., 2011). In halophilic
549 euryarchaea, an RHH family transcription factor, CdrS, plays a central role in the
550 regulation of the cell division. Similar to aCcr1 of *S. islandicus*, *cdrS* is essential in

551 *Haloferax volcanii* and could not be deleted. CdrS is a global transcriptional regulator,
552 controlling expression of *ftsZ*. It also regulates the expression of genes linked to other
553 metabolic and regulatory processes, likely allowing cells to properly coordinate growth,
554 division, and metabolic activity (Liao et al., 2021a, 2021b). CdrS binds upstream of the
555 promoters of *ftsZ1* and *dacZ* (encoding a diadenylate cyclase, DacZ), which
556 synthesizes the second messenger molecule c-di-AMP, and three genes related to
557 proteasome function (*cdc48d*, *panA*, and *psmB*) (Liao et al., 2021a; Liao et al., 2021b).
558 In another halophile, *Halobacterium salinarum*, the gene coding for the CdrS is co-
559 transcribed with the cell division gene *ftsZ2,* and the gene encoding CdrL, another
560 RHH transcription factor which binds the promoter of *cdrS-ftsZ* (Darnell et al., 2020).
561 Interestingly, in this haloarchaeon, the *cdrS* can be deleted and appears not to be
562 involved in the regulation of DacZ and proteasome proteins, which might explain its
563 dispensability (Darnell et al., 2020). The *cdrS-ftsZ2* locus is well conserved across the
564 Euryarchaeota, especially within the Halobacteria (Darnell et al., 2020) (Fig. S10),
565 suggesting a general cell division regulation mechanism in euryarchaea.

566 There are many obvious parallels between aCcr1 and CdrS. In particular, both aCcr1
567 and CdrS are small RHH transcription factors and although they are distantly related
568 at the amino acid sequence level, the modelled three-dimensional structures are very
569 similar (Fig. S1C). Furthermore, the aCcr1-box is similar to the most conserved part of
570 the putative CdrS binding motif (also a palindromic sequence) (Liao et al., 2021b).
571 Finally, CdrS and aCcr1 play equivalent roles in the control of cell cycle progression.
572 We hypothesize that the aCcr1/CdrS-mediated cell division regulation mechanism has
573 evolved before the divergence of archaeal lineages using the ESCRT-III-based and
574 FtsZ-based cell division systems.

575 Apart from *cdvA*, 11 other genes were repressed by aCcr1. We have confirmed that
576 the conserved aCcr1-box motif was responsible for aCcr1 binding to the *ePK1*
577 promoter. The ePK1 from *S. islandicus* and its homolog in *S. acidocaldarius* exhibited
578 DNA damage agent-dependent changes at transcriptional level or in phosphorylation
579 status (Gotz et al., 2007; Huang et al., 2020; Sun et al., 2018). Phosphorylation plays
580 a crucial role in the cell cycle regulation in eukaryotic cells, and could play a similar
581 role in archaea. For instance, repression of *ePK1* could regulate the cell cycle through
582 protein phosphorylation. Functions for the other 10 proteins for which the promoters
583 contain aCcr1-box include possible nutrient uptake related proteins (endoglucanase,
584 SiRe_0332, and thermopsin-like protease, SiRe_0691) and a predicted component of
585 anti-virus defence system ATPase (SiRe_0086) (Table 1). Further characterization of
586 the regulation of these genes by aCcr1 could help unravel the cell cycle regulation
587 network in Archaea.

588 Many aCcr1 homologs are present in the genomes of archaeal viruses (Fig. 8). Over-
589 expression of the aCcr1 homologs from the *Acidianus* two-tailed virus (ATV_gp29) and
590 *Sulfolobus* monocaudavirus 3 (SMV3_gp63) resulted in growth retardation and
591 appearance of enlarged cells with multiple chromosomes (Fig. 9). *Acidianus* two-tailed

virus and *Sulfolobus* monocaudavirus 3 are spindle-shaped viruses which also include genetically distant but morphologically similar *S. tengchongensis* spindle-shaped virus 1 (STSV1), *S. tengchongensis* spindle-shaped virus 2 (STSV2), *Acidianus* tailed spindle virus (ATSV), and *Sulfolobus* monocaudavirus 1 (SMV1), all members of the family *Bicaudaviridae* (Prangishvili et al., 2018). We previously reported a virus-induced cell enlargement of *S. islandicus* REY15A by SMV1 and STSV2, illuminating the inherent plasticity of *Sulfolobus* cells, which might be relevant for eukaryogenesis (Liu et al., 2021a). Although the regulators manipulating cell division in STSV2 and SMV1 are yet to be identified, the finding that ATV- and SMV3-encoded aCcr1 homologs induce cell enlargement suggests that a similar mechanism might be operating in STSV2- and SMV1-infected cells. By hijacking a key cell division regulator, viruses can manipulate the archaeal cell cycle, transforming the infected cell into a giant virion producing factory. A similar event might have also taken place in archaea ancestral to eukaryotes, whereby virus infection produced cells with sufficiently large volume, a prerequisite for eukaryogenesis.

Global transcriptional analysis revealed that transcription of aCcr1 and cell division proteins CdvA, ESCRT-III and Vps4 are cyclically controlled in *S. acidocaldarius* (Lundgren and Bernander, 2007). Interestingly, the peak of aCcr1 (Saci_0942) transcription was about 30 minutes after that for CdvA, but coincided with those of ESCRT-III and Vps4. In our transcriptomic analysis, a similar pattern was observed (Fig. 1B). Based on these results, we propose a scenario of cell division control by aCcr1 in *S. islandicus* REY15A. After cell division is initiated by CdvA, aCcr1 expression is activated by an unidentified factor, leading to a timely shut down of the CdvA expression (Liu et al., 2021b). This will prevent further recruitment of ESCRT-III to the membrane at the mid-cell and ensure that the cell division ring assembles only during the cytokinesis stage of the cell cycle. In summary, we have identified a key cell division regulator, a small RHH family protein aCcr1 that controls cell division in crenarchaea through repression of the early cell division protein in the cytokinesis machinery. This study open doors for further dissection of the cell cycle regulation network in archaea.

Acknowledgements

This work was supported by the National Key Research and Development Program of China (No. 2020YFA0906800), the National Natural Science Foundation of China (No. 31970546 and 31670061 to YS, 31970119 to JN, and 31771380 to QS) and the State Key Laboratory of Microbial Technology. Work in the MK laboratory was supported by a grant from Ville de Paris (Emergence(s) project MEMREMA). We would like to thank all the lab members of the CRISPR and Archaea Biology Research Centre for helpful discussions.

References

1. Altschul, S.F., Madden, T.L., Schaffer, A.A., Zhang, J., Zhang, Z., Miller, W., and Lipman, D.J. (1997). Gapped BLAST and PSI-BLAST: a new generation of protein database search programs. Nucleic Acids Res *25*, 3389-3402.
2. Bernander, R. (2000). Chromosome replication, nucleoid segregation and cell division in archaea. Trends Microbiol *8*, 278-283.
3. Bernander, R., and Poplawski, A. (1997). Cell cycle characteristics of thermophilic archaea. J Bacteriol *179*, 4963-4969.
4. Capella-Gutierrez, S., Silla-Martinez, J.M., and Gabaldon, T. (2009). trimAl: a tool for automated alignment trimming in large-scale phylogenetic analyses. Bioinformatics *25*, 1972-1973.
5. Caspi, Y., and Dekker, C. (2018). Dividing the Archaeal Way: The Ancient Cdv Cell-Division Machinery. Front Microbiol *9*, 174.
6. Chu, Y., Zhu, Y., Chen, Y., Li, W., Zhang, Z., Liu, D., Wang, T., Ma, J., Deng, H., Liu, Z.J.*, et al.* (2016). aKMT Catalyzes Extensive Protein Lysine Methylation in the Hyperthermophilic Archaeon Sulfolobus islandicus but is Dispensable for the Growth of the Organism. Mol Cell Proteomics *15*, 2908-2923.
7. Darnell, C.L., Zheng, J., Wilson, S., Bertoli, R.M., Bisson-Filho, A.W., Garner, E.C., and Schmid, A.K. (2020). The Ribbon-Helix-Helix Domain Protein CdrS Regulates the Tubulin Homolog ftsZ2 To Control Cell Division in Archaea. mBio *11*.
8. Deng, L., Zhu, H., Chen, Z., Liang, Y.X., and She, Q. (2009). Unmarked gene deletion and host-vector system for the hyperthermophilic crenarchaeon Sulfolobus islandicus. Extremophiles *13*, 735-746.
9. Dewachter, L., Verstraeten, N., Fauvart, M., and Michiels, J. (2018). An integrative view of cell cycle control in Escherichia coli. FEMS Microbiol Rev *42*, 116-136.
10. Dexl, S., Reichelt, R., Kraatz, K., Schulz, S., Grohmann, D., Bartlett, M., and Thomm, M. (2018). Displacement of the transcription factor B reader domain during transcription initiation. Nucleic Acids Res *46*, 10066-10081.
11. Diaz-Moralli, S., Tarrado-Castellarnau, M., Miranda, A., and Cascante, M. (2013). Targeting cell cycle regulation in cancer therapy. Pharmacol Ther *138*, 255-271.
12. Evans, T., Rosenthal, E.T., Youngblom, J., Distel, D., and Hunt, T. (1983). Cyclin: a protein specified by maternal mRNA in sea urchin eggs that is destroyed at each cleavage division. Cell *33*, 389-396.
13. Gabler, F., Nam, S.Z., Till, S., Mirdita, M., Steinegger, M., Soding, J., Lupas, A.N., and Alva, V. (2020). Protein Sequence Analysis Using the MPI Bioinformatics Toolkit. Curr Protoc Bioinformatics *72*, e108.
14. Galderisi, U., Jori, F.P., and Giordano, A. (2003). Cell cycle regulation and neural differentiation. Oncogene *22*, 5208-5219.
15. Gotz, D., Paytubi, S., Munro, S., Lundgren, M., Bernander, R., and White, M.F. (2007). Responses of hyperthermophilic crenarchaea to UV irradiation. Genome Biol *8*, R220.
16. Guindon, S., Dufayard, J.F., Lefort, V., Anisimova, M., Hordijk, W., and Gascuel, O. (2010). New algorithms and methods to estimate maximum-likelihood phylogenies: assessing the performance of PhyML 3.0. Syst Biol *59*, 307-321.
17. Guo, L., Brugger, K., Liu, C., Shah, S.A., Zheng, H., Zhu, Y., Wang, S., Lillestol,

R.K., Chen, L., Frank, J.*, et al.* (2011). Genome analyses of Icelandic strains of Sulfolobus islandicus, model organisms for genetic and virus-host interaction studies. J Bacteriol *193*, 1672-1680.

18. Happonen, L.J., Redder, P., Peng, X., Reigstad, L.J., Prangishvili, D., and Butcher, S.J. (2010). Familial relationships in hyperthermo- and acidophilic archaeal viruses. J Virol *84*, 4747-4754.
19. Hoffmann, L., Anders, K., Bischof, L.F., Ye, X., Reimann, J., Khadouma, S., Pham, T.K., van der Does, C., Wright, P.C., Essen, L.O.*, et al.* (2019). Structure and interactions of the archaeal motility repression module ArnA-ArnB that modulates archaellum gene expression in Sulfolobus acidocaldarius. J Biol Chem *294*, 7460-7471.
20. Huang, Q., Lin, Z., Wu, P., Ni, J., and Shen, Y. (2020). Phosphoproteomic Analysis Reveals Rio1-Related Protein Phosphorylation Changes in Response to UV Irradiation in Sulfolobus islandicus REY15A. Front Microbiol *11*, 586025.
21. Huang, Q., Mayaka, J.B., Zhong, Q., Zhang, C., Hou, G., Ni, J., and Shen, Y. (2019). Phosphorylation of the Archaeal Holliday Junction Resolvase Hjc Inhibits Its Catalytic Activity and Facilitates DNA Repair in Sulfolobus islandicus REY15A. Front Microbiol *10*, 1214.
22. Huang, Q., Zhong, Q., Mayaka, J.B.A., Ni, J., and Shen, Y. (2017). Autophosphorylation and Cross-Phosphorylation of Protein Kinases from the Crenarchaeon Sulfolobus islandicus. Front Microbiol *8*, 2173.
23. Imachi, H., Nobu, M.K., Nakahara, N., Morono, Y., Ogawara, M., Takaki, Y., Takano, Y., Uematsu, K., Ikuta, T., Ito, M.*, et al.* (2020). Isolation of an archaeon at the prokaryote-eukaryote interface. Nature *577*, 519-525.
24. Katoh, K., Rozewicki, J., and Yamada, K.D. (2019). MAFFT online service: multiple sequence alignment, interactive sequence choice and visualization. Brief Bioinform *20*, 1160-1166.
25. Kessler, A., Brinkman, A.B., van der Oost, J., and Prangishvili, D. (2004). Transcription of the rod-shaped viruses SIRV1 and SIRV2 of the hyperthermophilic archaeon sulfolobus. J Bacteriol *186*, 7745-7753.
26. Lemmens, L., Maklad, H.R., Bervoets, I., and Peeters, E. (2019). Transcription Regulators in Archaea: Homologies and Differences with Bacterial Regulators. J Mol Biol *431*, 4132-4146.
27. Lewis, M., and Stracker, T.H. (2021). Transcriptional regulation of multiciliated cell differentiation. Semin Cell Dev Biol *110*, 51-60.
28. Li, Y., Pan, S., Zhang, Y., Ren, M., Feng, M., Peng, N., Chen, L., Liang, Y.X., and She, Q. (2016). Harnessing Type I and Type III CRISPR-Cas systems for genome editing. Nucleic Acids Res *44*, e34.
29. Liao, Y., Ithurbide, S., Evenhuis, C., Lowe, J., and Duggin, I.G. (2021a). Cell division in the archaeon Haloferax volcanii relies on two FtsZ proteins with distinct functions in division ring assembly and constriction. Nat Microbiol *6*, 594-605.
30. Liao, Y., Vogel, V., Hauber, S., Bartel, J., Alkhnbashi, O.S., Maass, S., Schwarz, T.S., Backofen, R., Becher, D., Duggin, I.G.*, et al.* (2021b). CdrS Is a Global Transcriptional Regulator Influencing Cell Division in Haloferax volcanii. mBio *12*,

e0141621.
31. Lindas, A.C., and Bernander, R. (2013). The cell cycle of archaea. Nat Rev Microbiol *11*, 627-638.
32. Lindas, A.C., Karlsson, E.A., Lindgren, M.T., Ettema, T.J., and Bernander, R. (2008). A unique cell division machinery in the Archaea. Proc Natl Acad Sci U S A *105*, 18942-18946.
33. Liu, J., Cvirkaite-Krupovic, V., Baquero, D.P., Yang, Y., Zhang, Q., Shen, Y., and Krupovic, M. (2021a). Virus-induced cell gigantism and asymmetric cell division in archaea. Proc Natl Acad Sci U S A *118*.
34. Liu, J., Cvirkaite-Krupovic, V., Commere, P.H., Yang, Y., Zhou, F., Forterre, P., Shen, Y., and Krupovic, M. (2021b). Archaeal extracellular vesicles are produced in an ESCRT-dependent manner and promote gene transfer and nutrient cycling in extreme environments. ISME J *15*, 2892-2905.
35. Liu, J., Gao, R., Li, C., Ni, J., Yang, Z., Zhang, Q., Chen, H., and Shen, Y. (2017). Functional assignment of multiple ESCRT-III homologs in cell division and budding in Sulfolobus islandicus. Mol Microbiol *105*, 540-553.
36. Liu, Y., Makarova, K.S., Huang, W.C., Wolf, Y.I., Nikolskaya, A.N., Zhang, X., Cai, M., Zhang, C.J., Xu, W., Luo, Z*., et al.* (2021c). Expanded diversity of Asgard archaea and their relationships with eukaryotes. Nature *593*, 553-557.
37. Lundgren, M., and Bernander, R. (2007). Genome-wide transcription map of an archaeal cell cycle. Proc Natl Acad Sci U S A *104*, 2939-2944.
38. Minh, B.Q., Schmidt, H.A., Chernomor, O., Schrempf, D., Woodhams, M.D., von Haeseler, A., and Lanfear, R. (2020). IQ-TREE 2: New Models and Efficient Methods for Phylogenetic Inference in the Genomic Era. Mol Biol Evol *37*, 1530-1534.
39. Morgan, D.O. (1995). Principles of CDK regulation. Nature *374*, 131-134.
40. Moriscot, C., Gribaldo, S., Jault, J.M., Krupovic, M., Arnaud, J., Jamin, M., Schoehn, G., Forterre, P., Weissenhorn, W., and Renesto, P. (2011). Crenarchaeal CdvA forms double-helical filaments containing DNA and interacts with ESCRT-III-like CdvB. PLoS One *6*, e21921.
41. Peng, N., Han, W., Li, Y., Liang, Y., and She, Q. (2017). Genetic technologies for extremely thermophilic microorganisms of Sulfolobus, the only genetically tractable genus of crenarchaea. Sci China Life Sci *60*, 370-385.
42. Prangishvili, D., Bamford, D.H., Forterre, P., Iranzo, J., Koonin, E.V., and Krupovic, M. (2017). The enigmatic archaeal virosphere. Nat Rev Microbiol *15*, 724-739.
43. Prangishvili, D., Krupovic, M., and Ictv Report, C. (2018). ICTV Virus Taxonomy Profile: Bicaudaviridae. J Gen Virol *99*, 864-865.
44. Reimann, J., Lassak, K., Khadouma, S., Ettema, T.J., Yang, N., Driessen, A.J., Klingl, A., and Albers, S.V. (2012). Regulation of archaella expression by the FHA and von Willebrand domain-containing proteins ArnA and ArnB in Sulfolobus acidocaldarius. Mol Microbiol *86*, 24-36.
45. Samson, R.Y., Obita, T., Freund, S.M., Williams, R.L., and Bell, S.D. (2008). A role for the ESCRT system in cell division in archaea. Science *322*, 1710-1713.
46. Samson, R.Y., Obita, T., Hodgson, B., Shaw, M.K., Chong, P.L., Williams, R.L.,

763 and Bell, S.D. (2011). Molecular and structural basis of ESCRT-III recruitment to
764 membranes during archaeal cell division. Mol Cell *41*, 186-196.
765 47. Schreiter, E.R., and Drennan, C.L. (2007). Ribbon-helix-helix transcription factors:
766 variations on a theme. Nat Rev Microbiol *5*, 710-720.
767 48. Spang, A., Caceres, E.F., and Ettema, T.J.G. (2017). Genomic exploration of the
768 diversity, ecology, and evolution of the archaeal domain of life. Science *357*.
769 49. Sun, M., Feng, X., Liu, Z., Han, W., Liang, Y.X., and She, Q. (2018). An Orc1/Cdc6
770 ortholog functions as a key regulator in the DNA damage response in Archaea.
771 Nucleic Acids Res *46*, 6697-6711.
772 50. Tarrason Risa, G., Hurtig, F., Bray, S., Hafner, A.E., Harker-Kirschneck, L., Faull,
773 P., Davis, C., Papatziamou, D., Mutavchiev, D.R., Fan, C.*, et al.* (2020). The
774 proteasome controls ESCRT-III-mediated cell division in an archaeon. Science
775 *369*.
776 51. Vorontsov, E.A., Rensen, E., Prangishvili, D., Krupovic, M., and Chamot-Rooke, J.
777 (2016). Abundant Lysine Methylation and N-Terminal Acetylation in Sulfolobus
778 islandicus Revealed by Bottom-Up and Top-Down Proteomics. Mol Cell
779 Proteomics *15*, 3388-3404.
780 52. Werner F., Grohmann D. (2011) Evolution of multisubunit RNA polymerases in the
781 three domains of life. Nat Rev Microbiol. *9*, 85-98.
782 53. Westfall, C.S., and Levin, P.A. (2017). Bacterial Cell Size: Multifactorial and
783 Multifaceted. Annu Rev Microbiol *71*, 499-517.
784 54. Willis, L., and Huang, K.C. (2017). Sizing up the bacterial cell cycle. Nat Rev
785 Microbiol *15*, 606-620.Yen, C.Y., Lin, M.G., Chen, B.W., Ng, I.W., Read, N., Kabli,
786 A.F., Wu, C.T., Shen, Y.Y., Chen, C.H., Barilla, D.*, et al.* (2021). Chromosome
787 segregation in Archaea: SegA- and SegB-DNA complex structures provide
788 insights into segrosome assembly. Nucleic Acids Res *49*, 13150-13164.
789 55. Yue, L., Li, J., Zhang, B., Qi, L., Li, Z., Zhao, F., Li, L., Zheng, X., and Dong, X.
790 (2020). The conserved ribonuclease aCPSF1 triggers genome-wide transcription
791 termination of Archaea via a 3'-end cleavage mode. Nucleic Acids Res *48*, 9589-
792 9605.
793 56. Zaremba-Niedzwiedzka, K., Caceres, E.F., Saw, J.H., Backstrom, D., Juzokaite,
794 L., Vancaester, E., Seitz, K.W., Anantharaman, K., Starnawski, P., Kjeldsen, K.U.,
795 *et al.* (2017). Asgard archaea illuminate the origin of eukaryotic cellular complexity.
796 Nature *541*, 353-358.

Table 1. Summary of genes with >4 fold down-regulated at mRNA levels in the aCcr1 over-expression strain based on comparative transcriptomic analysis*

Gene identity	Protein function	Sis/pSeSD-aCcr1 vs Sis/pSeSD log2 Fold Change
SiRe_0624	Blue (type 1) copper domain-containing protein	-3.458533126
SiRe_0623	Uncharacterized membrane protein	-3.261849277
SiRe_0670	Zinc finger SWIM domain-containing protein	-3.153753639
SiRe_2056	Serine/threonine protein kinase	-3.077324891
SiRe_0332	Cellulase (endo 1,4 beta glucanase), putative (CelB)	-2.944384326
SiRe_0764	CRISPR-associated, Csa3a	-2.922021684
SiRe_2100	SedA, Membrane protein involved in DNA uptake	-2.918474234
SiRe_0019	Queuine/archaeosine tRNA-ribosyltransferase	-2.906286786
SiRe_0086	ATPase, predicted component of phage defense system	-2.817790738
SiRe_0018	Queuine tRNA-ribosyltransferase related protein	-2.789165379
SiRe_1173	**Cell division protein CdvA**	**-2.669806305**
SiRe_2057	Uncharacterized membrane protein	-2.249728764
SiRe_1917	AIR synthase related protein	-2.226944702
SiRe_0691	Thermopsin-like protease	-2.224399679
SiRe_1464	Uncharacterized protein	-2.069938647
SiRe_0269	Uncharacterized protein	-2.045724686
SiRe_1239	Zn-dependent alcohol dehydrogenase	-2.030511419

* The cell division protein CdvA is shown in bold.

Table 2. Distribution of aCcr1-box in the promoter of highly down-regulated genes in the aCcr1 overexpressing strain and CdvA homologs from other archaeal species*

Gene identity	Promoter Sequences (-50 - +3)
SiRe_0624	TAGGTTCCATTAATCACAAAATTTTTTAACCTATGTACTAAGTAATACGTATG
SiRe_2056	ATACACATTGGGCTAAATATTTTAAGTGTTACCAGTAAAATAGTAATACCATG
SiRe_0332	AATAGCATTAACCTACTAATTTTTTAAAATTGCCAAAGTAAGTAATACCTATG
SiRe_0018	ATTATTATAAATGAAGTTATAACCCGATAGTAATACCAATACCAGGAAAAATG
SiRe_0086	GCTAACGATTATATTTTATTCTGCTAAGTATTACCGTAGAGTGATCTGTAGTG
SiRe_0269	GAAAATACTTTCGTGAATCTCAGTAGTGTTTTTTAAGTAAAATTTCTGATATG
SiRe_1917	AATCGTGTGATGGGAAAAATATATTATAATGGTATTACATTTTGCGTTTAATG
SiRe_0691	AGCATTACTATAACAATATTTAAATATAACATGGTACTACCCTTTTACCCATG
SiRe_1464	CCATAAACCTTAGGATAAACGTTATAACTAGCTAATAAGTAGTACACGTAATG
SiRe_1173 (CdvA)	ATCTTTATAAGTATTACTTAAAAGACCAAATATTTTTGAGGAGTATTACCATG
Saci_1374 (CdvA)	AATTCTTATAAATATAATCATCATAGCTGATAACTTTGAGGAGTAATACCATG
Ahos_1333 (CdvA)	TAACCTTTTTAAATATTTTATCTCAACATGTAACTTTGAGGAGTATTACCATG
Mcup_0558 (CdvA)	TCCTTTTAAATCGTTCCAAACTTAACTTGTATTTTTGAGGAGTATTACCTATG
IC006_1093 (CdvA)	ATCCTTTTAAAGCGAAATACTTAACCTCTAGCTTTTGAGGAGTAATACCTATG
D1868_04805 (CdvA)	AATCCTTTTAAATAAATCATACTCAGCTGATAATTTTGAGGAGTAATACCATG

* The aCcr1 box sequences are underlined and highlighted in yellow (sense strand) or green (antisense strand). The translation start codes are shown in red. SiRe_0019, SiRe_0623, and SiRe_2057 are not listed because they are in the same operon with of SiRe_0018 and SiRe_0624, respectively, or shares a bidirectional promoter with SiRe_2056.

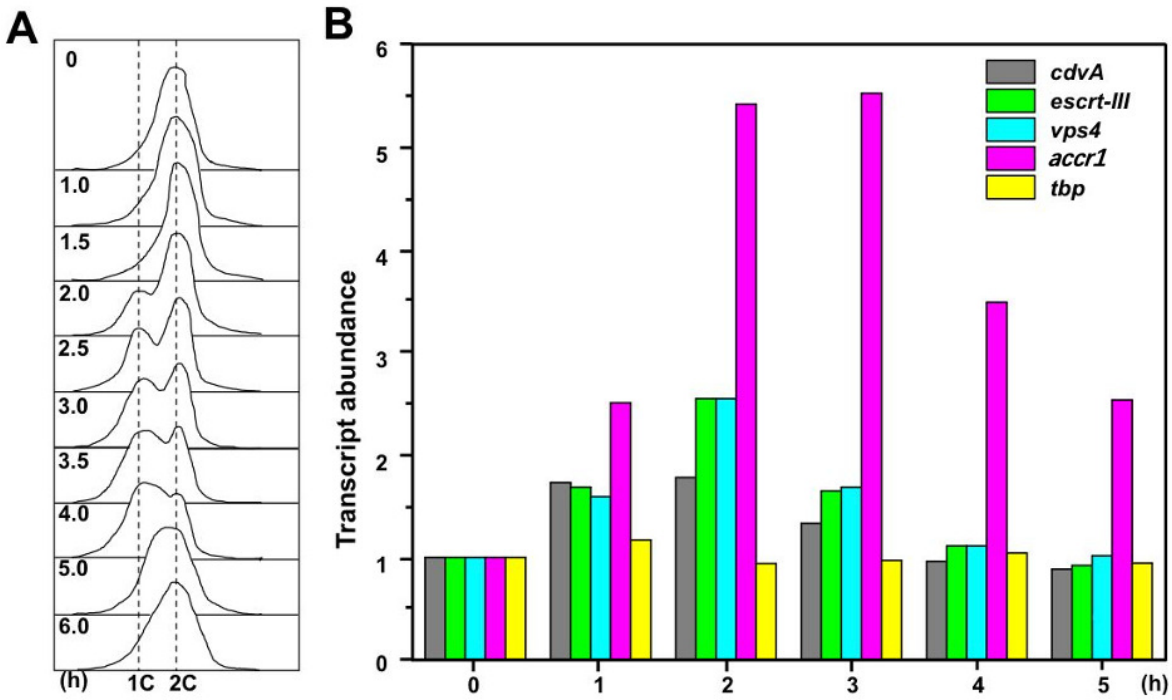

Figure 1. The gene *accr1* is cyclically transcribed. (**A**) Flow cytometry profiles of samples of a synchronized *S. islandicus* REY15A (E233S) culture in one cell cycle. The cells were synchronized at G2 phase after treated with 6 mM acetic acid for 6 h before released by removing the acetic acid. The cultures were collected at different time points (0, 1.0, 1.5, 2.0, 2.5, 3.0, 3.5, 4.0, 5.0, and 6.0 h) and subjected to flow cytometry analysis. Cells started to divide at 2.0 h as the appearance of cells with one copy of chromosome (1C) and the ratio of dividing cells reached the highest at about 3-3.5 h. As cell cycle proceeded, cells with two copies of chromosomes (2C) became dominant at 5 h. (**B**) Changes of transcription levels of *accr1* and the cell division genes based on the transcriptomic data of the synchronized cell culture. The cells were collected at 0, 1, 2, 3, 4, and 5 h after cell arrest release.

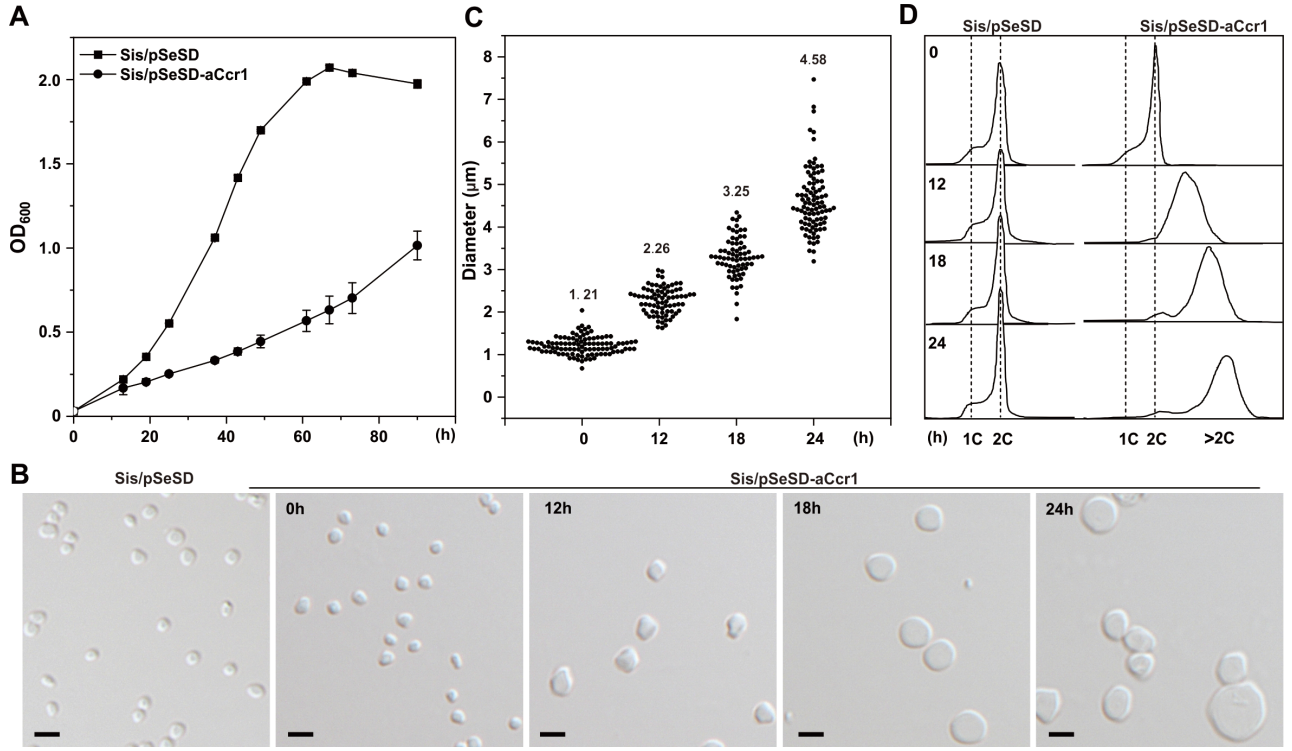

Figure 2. Overexpression of aCcr1 leads to remarkable cell enlargement. (A) Growth curves of cells over-expressing C-terminal His-tagged aCcr1. The cells were inoculated into 30 ml induction medium ATV to a final estimated OD_{600} of 0.03. The growth was monitored using spectrometer. Each value was based on data from three independent measurements. Cell harboring the empty plasmid pSeSD was used as a control. (B) Phase contrast microscopy of cells over-expressing aCcr1. Cells cultured in the induction medium were taken at different time points and observed under a NIKON-E microscope. Scale bars: 2 μm. (C) Cell size statistics of the data in (B). Cell cultures were sampled at the indicated time points and observed under the microscope. The diameters of ~100 cells were measured using ImageJ software for each culture repeat. (D) Flow cytometry analysis of the DNA content of Sis/pSeSD and Sis/pSeSD-aCcr1 cells cultured in MATV media.

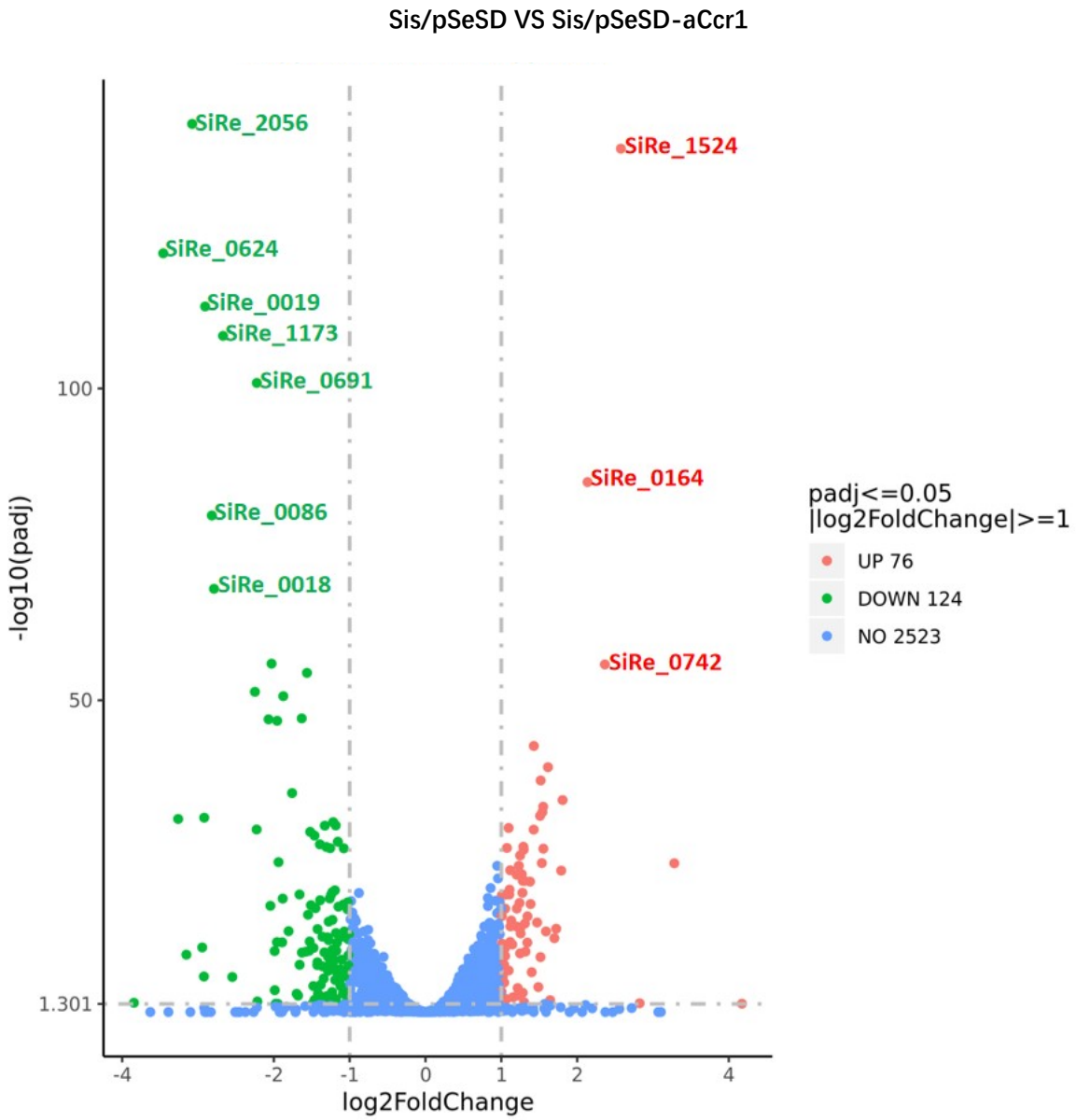

Figure 3. Volcano plot of differentially expressed genes in strain Sis/pSeSD-aCcr1 compared to the control Sis/pSeSD. X-axis, fold change in gene expression. Y-axis, significance of fold change. Genes exhibiting >2-fold (i.e. –1 > log2 > +1) up-and down-regulated with significance are highlighted in red and green, respectively, whereas those that showed a <2-fold change in differential gene expression or with no significance are shown in blue.

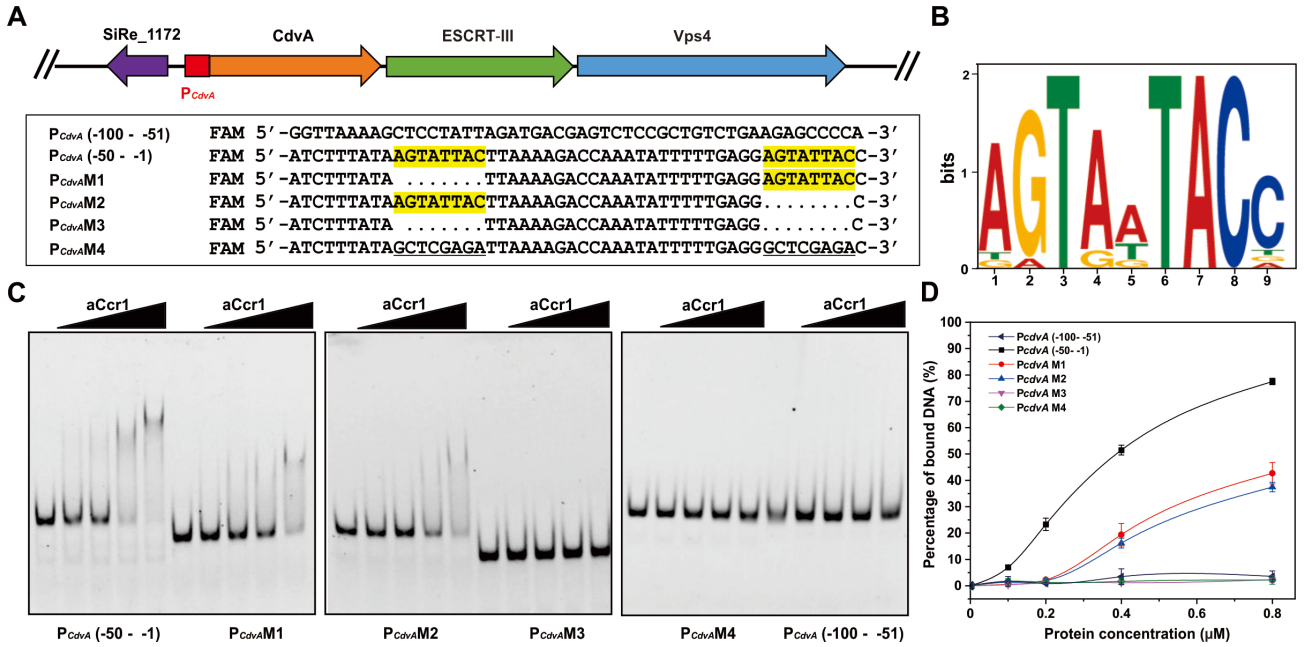

Figure 4. aCcr1 binds to the promoter of *cdvA* at the aCcr1-box motif. (**A**) Schematic organization of Cdv genes and *cdvA* promoter in the genome of *S. islandicus* REY15A. The sequences of the upper region (-100 - -51), lower region (-50 - -1) and its variant mutants used in the EMSA analysis are listed. The aCcr1-box motif is highlighted in yellow. Dots and the underlined indicate truncated and substitutive sequences, respectively. The oligonucleotides are labelled with FAM fluorescence at the 5'-ends for EMSA. (**B**) A conserved motif (designated as aCcr1-box) identified in the promoters of the highly repressed genes due to aCcr1 over-expression. A total of 15 promoter sequences (-60 - -1) of the down-regulated (>4 folds) genes plus promoter of *cdvA* from *Sulfolobus acidocaldarious* were used as the input for De Novo motif discovery by MEME server with the default setting. The height of the letter indicates the relative similarity to that of consensus one. (**C**) EMSA of aCcr1 binding to different regions of the promoter of *cdvA* and its mutants. The 5'FAM-labelled and corresponding complementary nucleotide sequences are listed in Table S2. The labelled oligonucleotides were annealed with the respective complementary strands as described in the Materials and Methods for the EMSA assay. The reaction was performed at 37℃ for 30 min and analysed on a 10% native PAGE (see "Materials and Methods"). Each reaction contained 2 nM of the FAM-labelled probe and 0, 0.1, 0.2, 0.4, or 0.8 μM aCcr1 protein. (**D**) Quantification of the results in (C). The values were obtained from three independent experiments. Error bars indicate standard deviation.

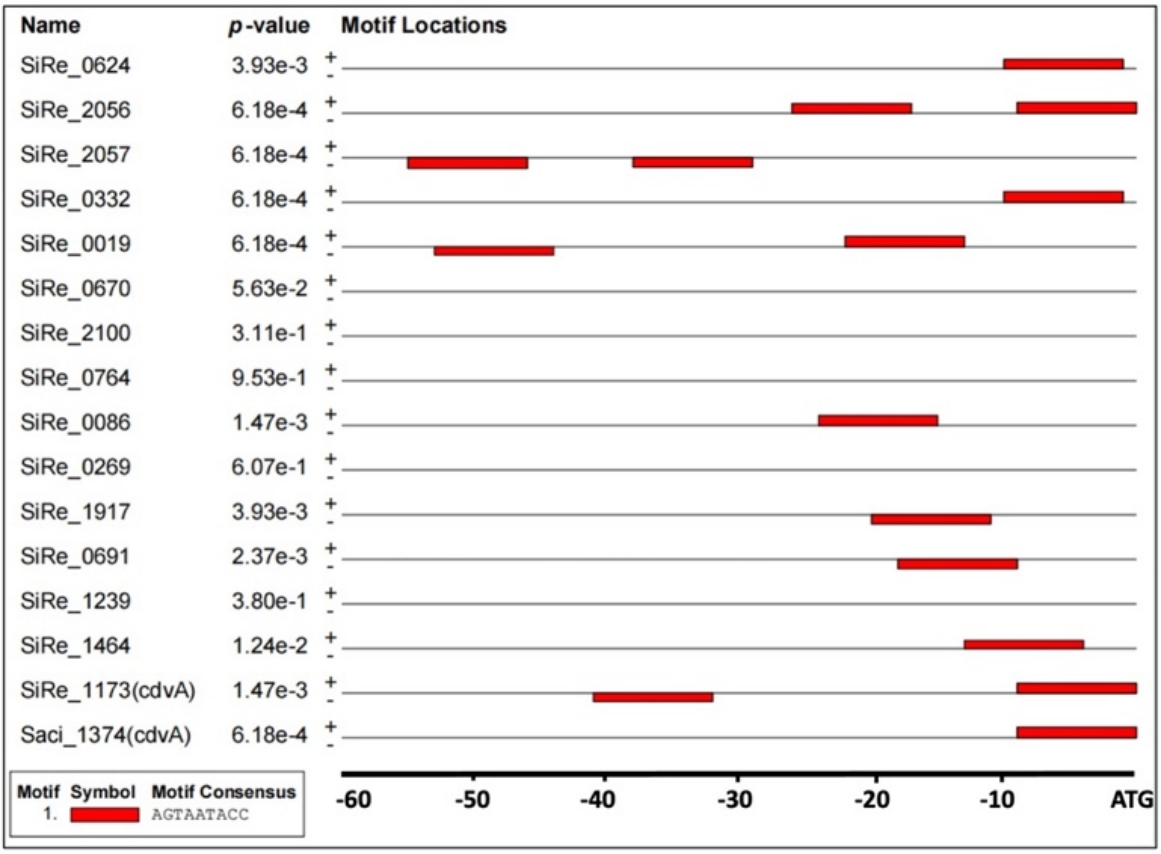

Figure 5. Distribution of aCcr1-box in the highly repressed gene promoters. "+" and "–"represent coding and non-coding strands, respectively.

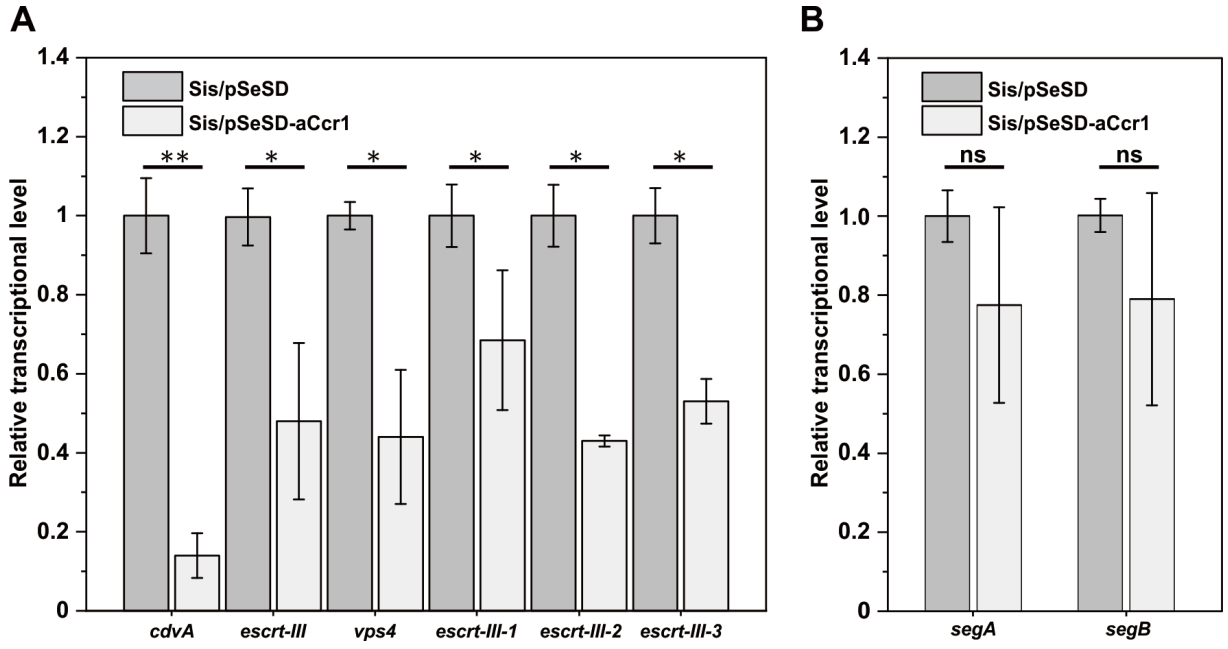

Figure 6. The expression of cell division genes is down regulated and that of the chromosome segregation genes is unchanged in the aCcr1 over-expression cells. Quantitative PCR (qPCR) analysis of the expression of cell division (**A**) and chromosome segregation genes (**B**) in aCcr1 over-expression cell in comparison with E233S cell carrying the empty vector (Sis/pSeSD). Cell cultures were sampled and analysed after 12 hours of arabinose induction. The 16S rRNA was used as the reference. The transcription levels of the target genes in the control strain (Sis/pSeSD) were defined as 1 (grey). ∗, P value<0.05; ∗∗, P value<0.01; ns, not significant. Error bars represent standard deviation from three independent repeats.

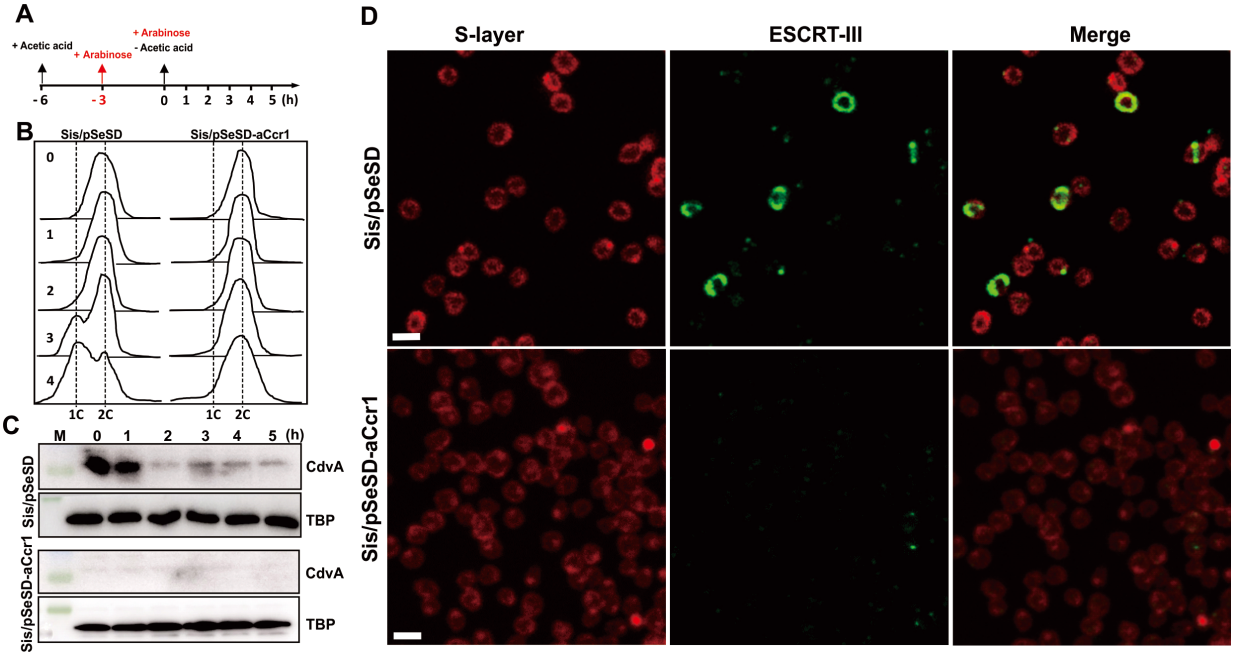

Figure 7. Over-expression of aCcr1 stalls cell division and impairs the ESCRT-III contractile ring formation. (**A**) Schematic showing the cell synchronization and induction of aCcr1 over-expression with arabinose (0.2%). Time for acetic acid treatment and arabinose induction are indicated. E233S containing the empty plasmid (Sis/pSeSD) was used as a control. (**B**) Flow cytometry profiles of DNA content distribution of cells 0-4 hrs after acetic acid removal. (**C**) Western blotting using anti-CdvA antibody in strain Sis/pSeSD-aCcr1 and the control at 0-5 hrs after acetic acid removal. TBP (TATA-box binding protein) was used as a loading control. The conditions for the Western blotting were as described in the Materials and Methods. Two gels and blots were used for each antibody with the same cell sample preparations and detection, except for CdvA, where 4 minutes was taken for exposure instead of 40 seconds. (**D**) Immuno-fluorescence microscopy showing the formation of contractile rings using the primary antibody against ESCRT-III (CdvB) and goat anti-rabbit secondary antibody Alexa Fluor® 488. The S-layer was stained with Concanavalin A, Alexa Fluor 647 Conjugate. Shown are representative images. M, molecular size marker.

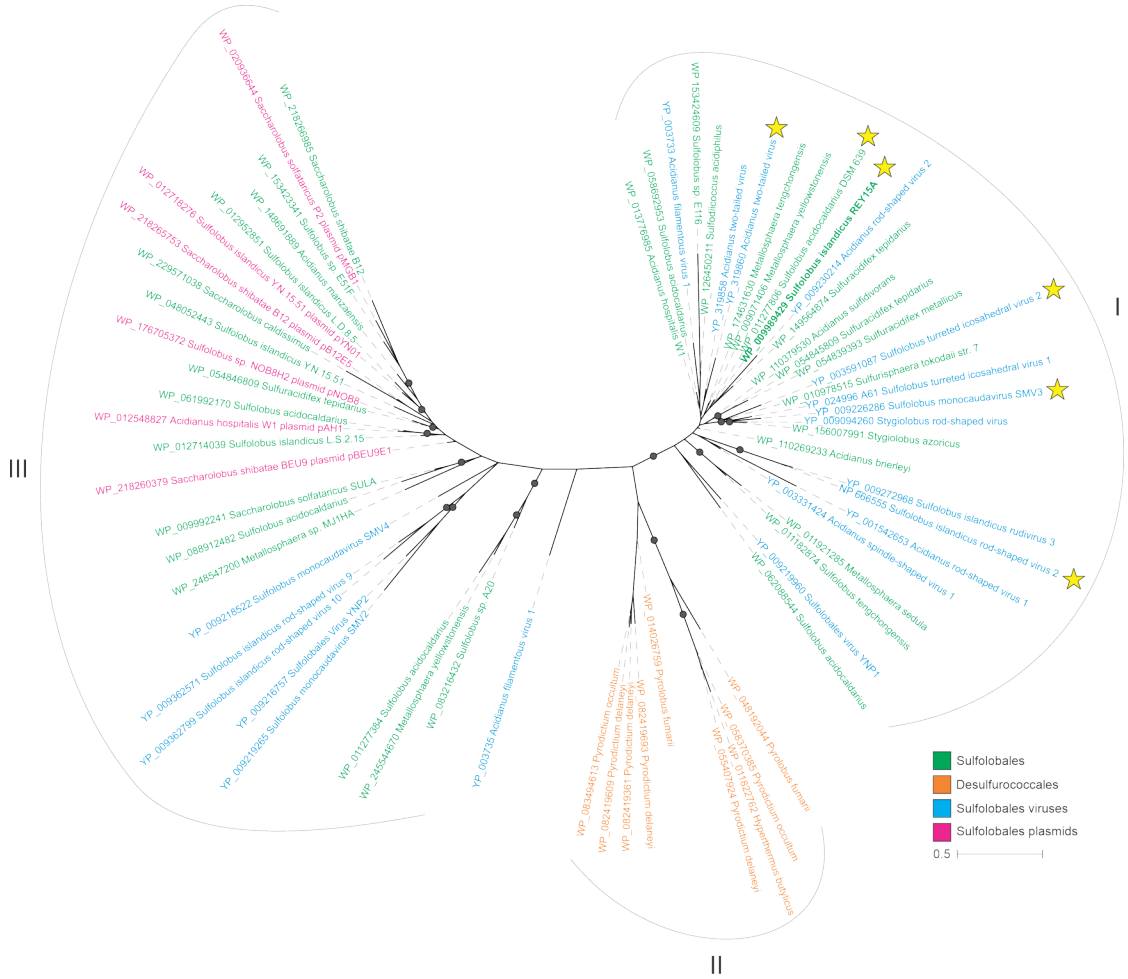

Figure 8. aCcr1 homologs are widely distributed in Sulfolobales and Desulfurococcales as well as in the plasmids and viruses of Sulfolobales. aCcr1 homologs were collected by PSI-BLAST. The collected sequences were then clustered using MMseq2. The sequences were aligned using MAFFT v7 and the resultant alignment trimmed using trimal. Phylogenetic analysis was performed using IQ-Tree and the branch support was assessed using SH-aLRT. The details of the analysis were listed in the Materials and Methods. The aCcr1 homologs investigated in this study were indicated with the yellow stars.

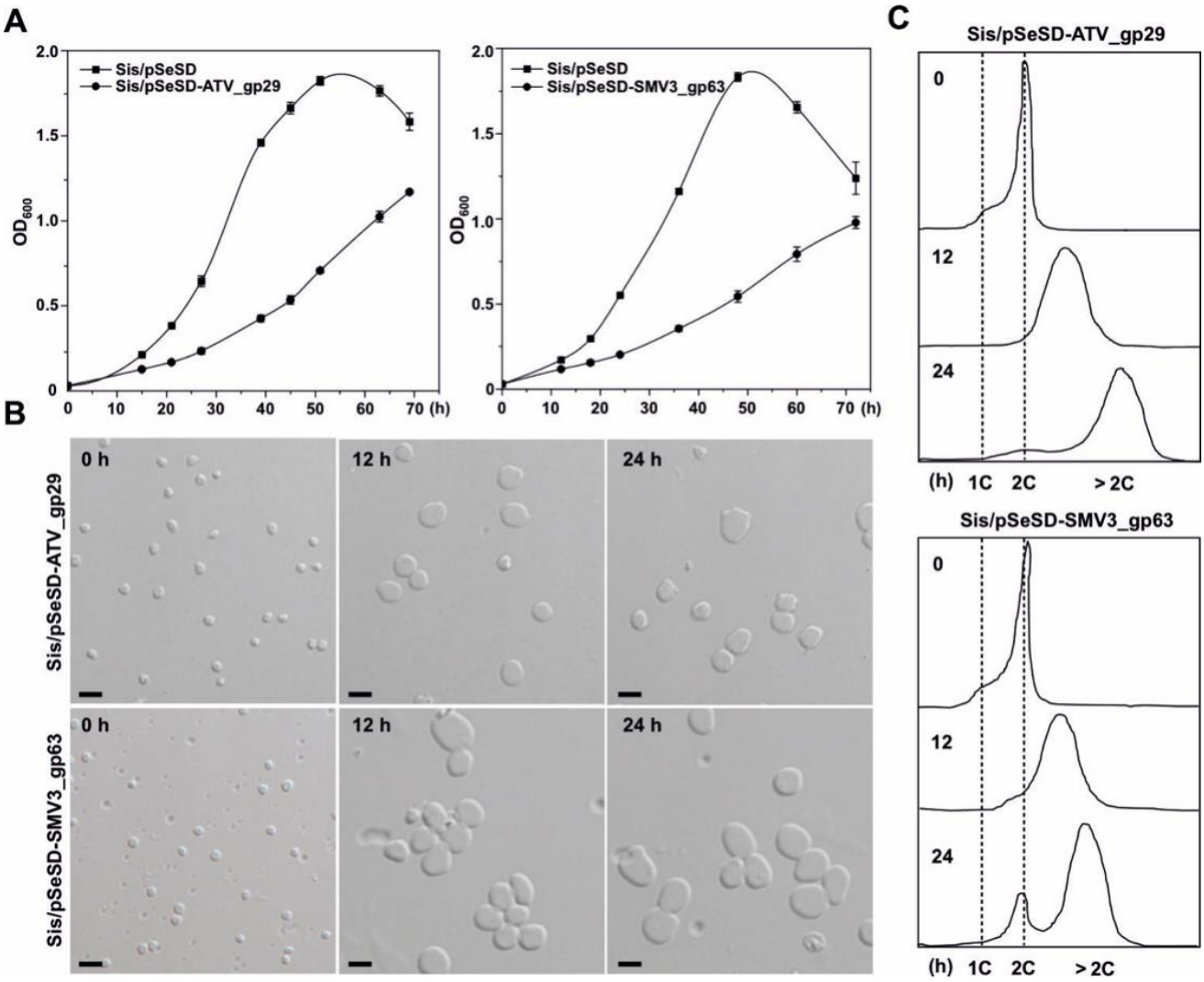

Figure 9. Cells with over-expression of the aCcr1 homologs, ATV_gp29 from *Acidianus* Two-tailed Virus and SM3_gp63 from *Sulfolobus* monocadauvirus 3 have similar phenotype as those with over-expression of SisCcr1. (**A**) Growth curves of cells Sis/pSeSD-ATV_gp29 and Sis/pSeSD-SMV3_gp63 cultured in induction medium ATV. The cells were inoculated into 30 ml medium to a final estimated OD_{600} of 0.03 and the growth was monitored using spectrometer. Each value was based on data from three independent repeats. Cell harboring the empty plasmid pSeSD was used as a control. (**B**) Phase contrast microscopy and (**C**) flow cytometry of cells over-expressing ATV_gp29 and SMV3_gp63. Cells cultured in medium ATV were taken at different time and observed under an inverted fluorescence microscope for DNA content using an ImageStreamX MarkII Quantitative imaging analysis flow cytometry (Merck Millipore, Germany). Scale bars: 2 μm.